

SIMULATION RESEARCH ON ONAN TRANSFORMER WINDING TEMPERATURE FIELD BASED ON TEMPERATURE RISE TEST

by

**Dongping XIAO^{a*}, Ruiyang XIAO^a, Fan YANG^a, Cheng CHI^a,
Mingsheng HUA^a, and Chun YANG^b**

^a State Key Laboratory of Power Transmission Equipment and
System Security and New Technology (Chongqing University), Chongqing, China

^b Xi'an Xidian Transformer Co.Ltd, Xi'an, China

Original scientific paper

<https://doi.org/10.2298/TSCI211127047X>

Studying the oil-natural-air-natural (ONAN) transformer's temperature field distribution characteristics and hot spot temperature rise during operation is a key step to evaluate the thermal insulation life of this type of transformer. Firstly, considering the transverse oil passages between the windings and the guiding effect of the oil baffle on the oil flow, this paper takes 35 kV ONAN transformer windings as the research object, which establishes the corresponding electromagnetic-thermal-fluid coupling model and uses the finite element method to calculate the overall distribution of the internal winding temperature field. The calculation results show that when the ONAN transformer reaches thermal equilibrium, the axial temperature distribution of the windings is extremely uneven due to the influence of the transformer oil flow rate, whose difference between both ends is as high as 17.4 °C. However, the existence of the oil baffle increases the flow velocity of the inter-turn transverse oil passage to 12 times of the original. Affected by this, the oil temperature difference between the two ends of the oil baffle is as high as 2.42 °C. Secondly, this paper conducted a short-circuit temperature rise test on the test prototype, and selected the different axial heights (18%, 72%, 96%, etc.) of the windings on both sides of the transformer as the characteristic sample points for embedding temperature measurement fiber for real-time temperature monitoring. After comparison, it is found that the simulation calculation is basically consistent with experiment data, and the relative error of the two is less than 3.3%.

Key words: *thermal insulation life, ONAN transformer,
temperature measurement fiber, temperature rise test ,
electromagnetic-thermal-fluid coupling model,
hot spot temperature rise*

Introduction

With the growth of my country's social economy, the power load-intensive areas continue to increase, and the transmission and distribution system has entered a period of high density construction [1]. Among them, oil-immersed power transformers are the core equipment of power transmission and distribution, and their operational reliability is not only related to their own insulation characteristics and service life, but also related to the safety and stability of the power system [2]. In recent years, the power supply capacity of oil-immersed transformers has continued to increase. However, due to the limitations of site size or cost, the structural size of

* Corresponding author, e-mail: xiaodongping@cqu.edu.cn

the transformer has not been increased simultaneously, which has aggravated the local overheating phenomenon. Therefore, the power supply accident of the power system occurs occasionally result from the high temperature of the transformer hot spot [3]. When the temperature rise of the hot spot exceeds the temperature rise limit of the transformer, it will accelerate aging of the insulation material and even cause insulation breakdown [4]. In addition, the temperature gradient of the upper and lower layers of the ONAN transformer windings is large, resulting in a large difference in the degree of thermal aging of the oil paper at both ends. Therefore, in order to realize the collaborative optimization of ONAN transformer capacity and design margin, ensuring its good insulation life, it is necessary to study the temperature field distribution of the internal winding of this type of transformer.

Until now, corresponding researches have been carried out on the temperature characteristics of oil-immersed transformers. In [5, 6] has realized the rapid prediction of the highest temperature rise of oil-immersed transformers through thermoelectric analogy, but it fails to determine the specific location of the hot spots and distribution law of temperature field inside the transformer. In [7] completed the hot spot inversion in the tank according to the flow line of the transformer oil, and realized the location of the hot spot under non-implanted temperature measurement. It pointed out that the temperature concentration area of the transformer is under the top of the winding, while the selection method of the main flow is so simple, having a certain degree of subjective randomness, that it is not suitable for hot-spot calculations of complex transformers;. In [8-10] used numerical analysis to construct the electromagnetic-thermal-fluid coupling model of ONAN transformer, and solves it through multiple iterations. The numerical analysis realized the calculation of the temperature field of the transformer's internal windings and the location of hot spots. But from a numerical point of view, the calculation cost of this type of model is too large, especially the existence of millimeter-level structures such as insulating paper has strict requirements for precision grids, which increased the difficulty of meshing and easily caused the stiffness matrix to not converge. In [11] pointed out that under the condition of controlling the Richardson number, the 2-D axisymmetric transformer model can be equivalent to the 3-D model, but the numerical models in this type of literature ignored the hysteresis of the oil flow between the transverse oil passages of the windings and guiding role of the oil baffle on the heat dissipation efficiency of the winding wire cake. The cylindrical treatment of the windings makes the calculated temperature of the middle of the winding higher and the temperature difference between the ends of the winding smaller, causing the hot spot location discrepancy between the numerical results and actual situation.

Therefore, in order to study the temperature field distribution characteristics of the ONAN transformer, on the one hand, this paper takes an 800 kVA/35 kV ONAN transformer as the research object, which establishes the transformer electromagnetic-thermal-fluid coupling 2-D axisymmetric model and obtains oil velocity distribution cloud diagram of the transformer through finite element calculation, on the other hand, the short-circuit temperature rise test of the actual prototype is carried out in this paper, using the temperature-measuring fiber to obtain the temperature rise data of the corresponding characteristic points in the thermal balance. The experimental data verified the accuracy of the electromagnetic-thermal-fluid coupling model of the ONAN transformer proposed in this paper. This research provides the hot spot assessment and insulation optimization design of the ONAN transformer for reference.

The ONAN transformer multi-physical field coupling calculation

Electromagnetic-thermal-fluid field coupling control equation

The internal heat source of the ONAN transformer mainly comes from the ohmic loss generated by the windings on both sides, and the heat is transferred to the transformer oil through heat convection. The heated transformer oil contacts the transformer tank wall and the radiating fins at both ends under the action of thermal buoyancy, and transfers the heat to the air around the transformer through thermal convection achieve natural heat dissipation. The cooled transformer oil returns to the bottom of the tank and is heated again to perform a new cycle of heat dissipation until the transformer reaches a dynamic thermal balance.

The ohmic loss generated by the winding is the main heat source, and its calculation formula is eq. (1). Considering the reverse coupling effect of temperature on the winding resistivity, in order to refine the calculation results, it is necessary to correct the winding loss according to the change in the temperature of the winding material [12]:

$$p_c = \rho(T) |\mathbf{J}^2| \quad (1)$$

$$\rho(T) = \rho_0 [1 + \beta(T - T_0)] \quad (2)$$

where p_c is the winding ohmic loss density, ρ_0 – the resistivity when the temperature of the wire is T_0 , and β are the conductor temperature coefficient, which is 0.00393 in this article.

Inside the transformer, the transformer oil is heated to expand and its density is reduced. Under the action of thermal buoyancy, the heat is transferred to the surrounding environment to achieve heat dissipation. Considering that the Mach number of the fluid is small, the transformer oil can be regarded as an incompressible fluid. The flow process of the oil flow in the steady-state is controlled by the mass, momentum and energy conservation equations [13]:

$$\frac{1}{r} \frac{\partial(ru)}{\partial r} + \frac{\partial v}{\partial z} = 0 \quad (3)$$

$$\begin{aligned} u \frac{\partial u}{\partial r} + v \frac{\partial u}{\partial z} &= -\frac{1}{\rho} \frac{\partial p}{\partial r} + \mu_k \left[\frac{\partial}{\partial r} \left(\frac{1}{r} \frac{\partial(ru)}{\partial r} \right) + \frac{\partial^2 u}{\partial z^2} \right] \\ u \frac{\partial v}{\partial r} + v \frac{\partial v}{\partial z} &= -\frac{1}{\rho} \frac{\partial p}{\partial z} - g + \mu_k \left[\frac{1}{r} \frac{\partial}{\partial r} \left(r \frac{\partial v}{\partial r} \right) + \frac{\partial^2 v}{\partial z^2} \right] \end{aligned} \quad (4)$$

$$\frac{\nabla(\rho c_p u T)}{\partial r} + \frac{\nabla(\rho c_p v T)}{\partial z} - \lambda \frac{\partial^2 T}{\partial z^2} - \lambda \frac{1}{r} \frac{\partial}{\partial r} \left(r \frac{\partial T}{\partial r} \right) = p_s = p_c = \rho_0 [1 + \beta(T - T_0)] |\mathbf{J}^2| \quad (5)$$

Equation (3) is the momentum conservation equation, u and v are the radial velocity and axial velocity of the transformer oil speed, respectively. Equation (4) is the Navier-Stokes equation, that is, the momentum conservation equation. Equation (5) is the energy conservation equation, p_s is the heat source of the winding, and c_p , μ_k are the temperature-dependent specific heat capacity and dynamic viscosity of the transformer oil, respectively.

The static pressure, p , in the fluid boundary-layer consists of two parts: the hydrostatic pressure, p_∞ , at the reference point and the dynamic pressure, p_r , caused by the fluid movement. Because $p_\infty \gg p_r$ [14]:

$$\frac{\partial p}{\partial z} = -\rho_\infty g \quad (6)$$

Among them, ρ_∞ is the transformer oil density at the reference point. Insert eq. (6) into eq. (4):

$$u \frac{\partial v}{\partial r} + v \frac{\partial v}{\partial z} = \frac{1}{\rho} \rho_\infty g - g + \mu_k \left[\frac{1}{r} \frac{\partial}{\partial r} \left(r \frac{\partial v}{\partial r} \right) + \frac{\partial^2 v}{\partial z^2} \right] = \frac{g}{\rho} (\rho_\infty - \rho) + \mu_k \left[\frac{1}{r} \frac{\partial}{\partial r} \left(r \frac{\partial v}{\partial r} \right) + \frac{\partial^2 v}{\partial z^2} \right] \quad (7)$$

where $(\rho_\infty - \rho)$ is the thermal buoyancy. Because the oil flow in the ONAN transformer has a small flow rate and the density of the fluid does not change significantly, in order to reduce the degree of non-linearity in solving the problem to avoid the problem of decreased convergence caused the density evaluation, this article will introduce Boussinesq approximation:

- only consider the change of fluid density in the buoyancy term ρg of the equation, and the other terms are set as constants and
- the fluid density difference is proportional to the temperature difference. Therefore, the fluid volume expansion coefficient α :

$$\alpha = \frac{1}{V} \left(\frac{\partial V}{\partial T} \right)_p = - \frac{1}{\rho} \left(\frac{\partial \rho}{\partial T} \right)_p \approx \frac{1}{\rho} \frac{\rho_\infty - \rho}{T - T_\infty} \quad (8)$$

where V is the volume of the fluid boundary-layer. Substitute eq. (8) into eq. (7):

$$u \frac{\partial v}{\partial r} + v \frac{\partial v}{\partial z} = \alpha g (T - T_\infty) + \mu_k \left[\frac{1}{r} \frac{\partial}{\partial r} \left(r \frac{\partial v}{\partial r} \right) + \frac{\partial^2 v}{\partial z^2} \right] \quad (9)$$

The physical parameters of transformer oil are shown in tab. 1. The multi-field coupling mechanism in the ONAN transformer is shown in fig. 1.

Table 1. Transformer oil physical parameters

Material properties	Value
Density, ρ [kgm^{-3}]	$1080.23 - 0.712T$
Thermal conductivity, λ [$\text{Wm}^{-1}\text{K}^{-1}$]	$0.20309 - 7.01 \cdot 10^{-5}T$
Dynamic viscosity, μ [$\text{Pa}\cdot\text{s}$]	$0.08467 - 4 \cdot 10^{-4}T + 5 \cdot 10^{-7}T^2$
Specific heat capacity, c_p [$\text{Jkg}^{-1}\text{K}^{-1}$]	$1744.23 + 4.21T$

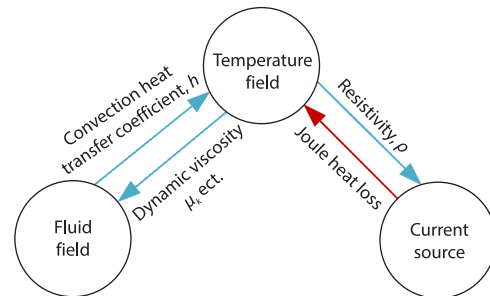
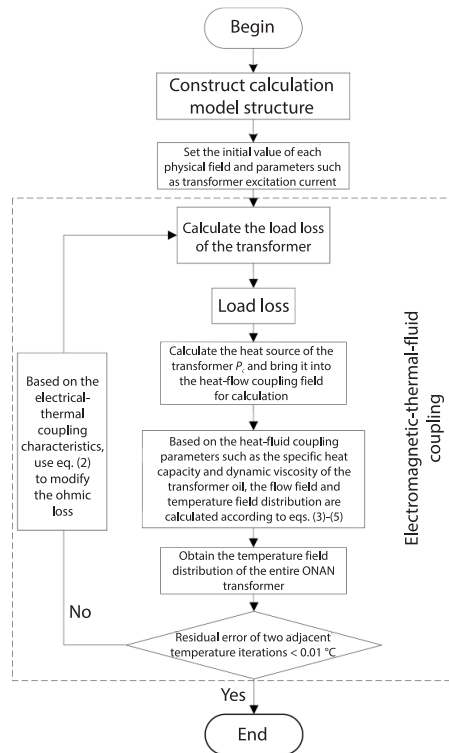


Figure 1 Multi-field coupling mechanism in ONAN transformer

Electromagnetic-thermal-fluid field coupling analysis

In this paper, the sequential coupling method is used to study the internal temperature field distribution characteristics of the ONAN transformer windings under the electromagnetic-thermal-fluid coupling field. The finite element method is used to solve the winding loss distribution, and the calculated loss value is used as the heat source load calculated by the heat-flow coupling module to obtain the preliminary temperature distribution characteristics in the ONAN transformer. According to eq. (2), the load loss is corrected and the flow is recalculated. The thermal coupling field is calculated iteratively in this way until the residual value of the two adjacent temperature iterations is lower than 0.01°C . The flow chart of the numerical calculation of the temperature field of the ONAN transformer in this paper is shown in fig. 2.

Figure 2. Flow chart of numerical calculation of temperature field of ONAN transformer



Model building

In this paper, based on the actual prototype structure parameters provided by the transformer manufacturer, a 35kV transformer winding calculation model as shown in fig. 3 is established. The windings on both sides are continuously wound. The high voltage coil has a total of 2933 turns and is composed of 72 wire cakes, and the low voltage coil has a total of 2×440 turns and is composed of 50 wire cakes. The length r_h of the high voltage winding wire cake is 61.5 mm, the width z_h is 4.1 mm, the width of the transverse oil passage between turns $z_{h,duct}$ is 2.18146 mm, the length of the low voltage winding wire cake r_l is 37 mm, the width z_l is 7 mm, and the width of the transverse oil passage between turns $z_{l,duct}$ is 2.24665 mm, and the thickness of the insulating paper tube is 2 mm. There are three oil baffles on both sides of the windings for guiding and shunting, forming a total of 8 guiding zones. The physical parameters of the specific structural parameters of the transformer are shown in tab. 2.

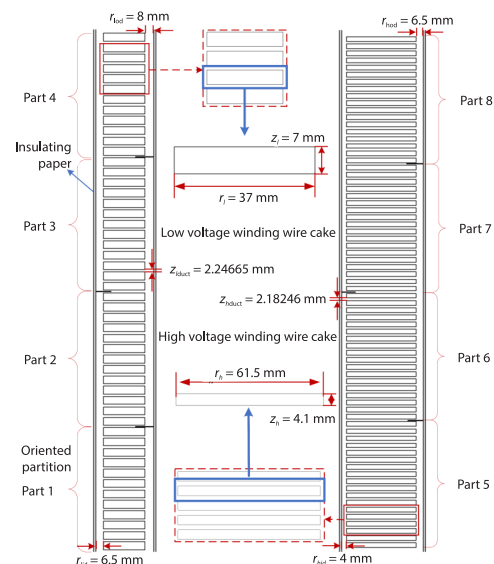


Figure 3. The 35 kV transformer winding calculation model

Table 2. Specific structural parameters of ONAN transformer

Parameter	Value	Parameter	Value
Capacity [kVA]	800	Core diameter [mm]	210
Frequency [Hz]	50	Iron core height [mm]	640
Cooling method	ONAN	Number of turns of high voltage winding coil	2933
Voltage level [kV]	30/10.5	Number of turns of low voltage winding coil	2×440
High voltage current [A] winding current [A]	11.43	Low voltage current [A] winding current [A]	76.2

Numerical calculation results and analysis

Figure 4(a) is a cloud diagram of the winding temperature field distribution of a 35 kV ONAN transformer, from which we can see:

- The overall temperature of the windings on both sides shows an upward trend. This is because the continuous increase in oil temperature affected by heat convection lead to a decrease in the temperature difference between oil and cake, which further reduces the heat dissipation of the winding wire cake. Therefore, the overall temperature of the windings on both sides shows an upward trend.

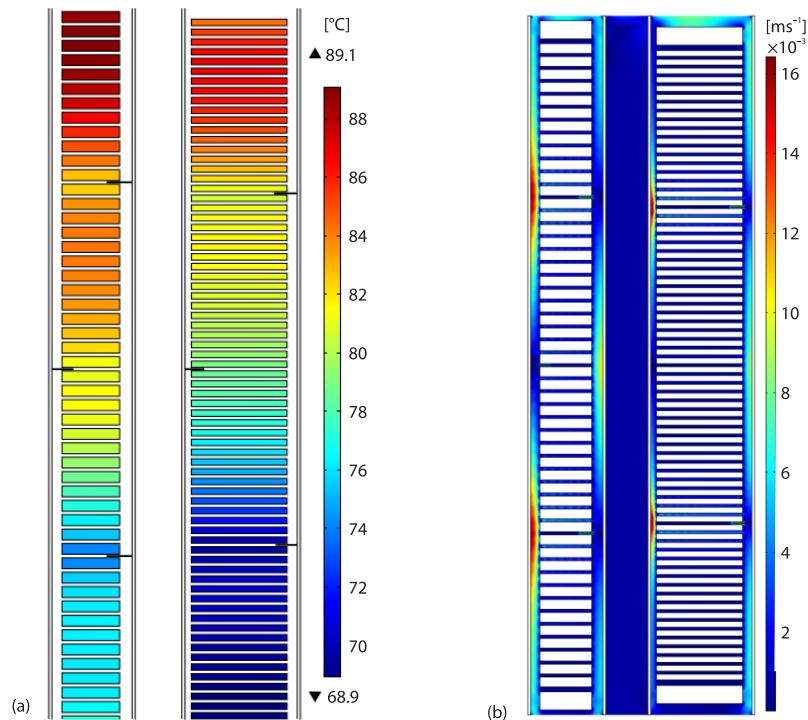


Figure 4. Distribution cloud diagram of physical field;
(a) winding temperature distribution cloud map and
(b) transformer oil velocity distribution cloud map

- The hot spot of the ONAN transformer is located at the third wire cake below the top of the low voltage winding (*i.e.* 96% of the axial height of the winding), the highest temperature is 89.1 °C. The hot spot temperature of the high voltage side winding is 86.6 °C, located at 93% of the axial height. The temperature difference between the upper and lower windings on both sides is 15.0 °C and 17.8 °C, respectively. Since the low voltage winding is on the inside and close to the core, dissipation condition of the low voltage winding is inferior to that of the high voltage side winding, transformer hot spots appear at low voltage. In consequence of heat convection, the oil temperature shows a continuous increase trend, which leads to a decrease in the temperature difference between oil and windings. The previous phenomenon further reduces the heat dissipation of the winding cakes, but the heat dissipation environment at the winding end is good, therefore, the temperature of the wire cake drops to a certain extent. In summary, the transformer hot spot is located under the end of the low voltage winding.
- In each oriented partition of the winding, the temperature of the winding wire cake shows a trend of first rising and then falling. The specific value changes are shown in fig. 10(d).

The oil flow in the transverse oil passage between winding turns is slow, and there is a phenomenon of oil flow hysteresis, which can be shown in fig. 4(b). The existence of the oil baffle can obstruct the movement of the oil flow in the axial oil passage in a forced driving manner, so that the oil flow can only exchange heat with the line cake through the transverse oil passage as the main flow path. In the case of a certain flow rate, the narrowing of the oil passage will speed up the flow rate of the oil flow, and further optimize the heat dissipation effect of the transformer oil. Figures 5 and 6 quantify the influence of the oil baffle on the oil

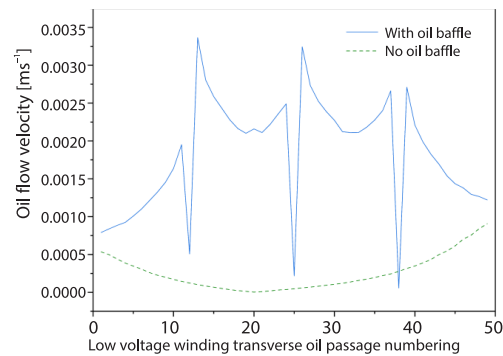


Figure 5. The internal flow velocity distribution diagram of the oil passage of the ONAN transformer winding

flow. Compared with the horizontal oil passage without the oil baffle plate, the existence of the oil baffle plate increases the flow velocity of the center point of the horizontal oil pas-

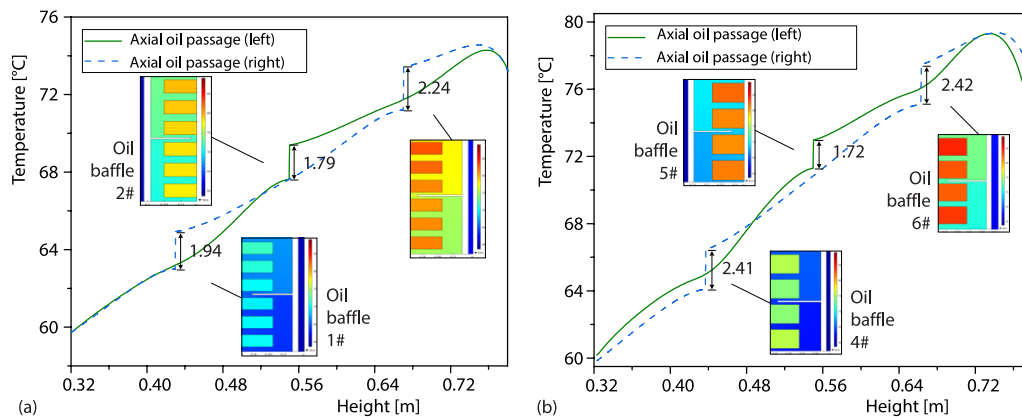


Figure 6. Comparison of oil temperature data of the axial oil passages on both sides of the ONAN transformer winding; (a) low voltage winding and (b) high voltage winding

sage by 0.5-12 times compared with the former. The horizontal oil passage close to the oil baffle plate has the strongest amplification effect, so oil temperature difference between the two ends of the oil baffle can reach 2.42 °C, and the highest temperature in every oriented partition is located at 2-3 line cakes below the top oil baffle.

The 35 kV ONAN transformer temperature rise test

Test design

The temperature rise test is one of the factory tests of the transformer, and it is also the type test that takes the longest time and requires the largest power supply capacity among all routine tests and type tests of the transformer. The purpose is to test whether there is local overheating in the transformer under the specified conditions by simulating the thermal characteristics of the transformer under rated operation and over-nameplate load conditions [15].

According to the guidance requirements of GB/T 7714-2015, in order to minimize the power output capacity required for the temperature rise test and ensure the safety of the test operation, this experiment adopts the short-circuit method: the low voltage side winding is short-circuited with a metal plate and high voltage winding is applied power frequency AC power, adjust the power supply voltage to increase the current in the high voltage winding to 1.0 (standard unit

value) and keep it until the temperature change rate of the monitoring point is lower than 1 °C per hour, the operation is completed and the experiment is ended. The whole experiment lasts for 8 hours and 20 minutes. The principle wiring diagram and the experiment wiring diagram at the scene are shown in figs. 7 and 8. During the test, the room temperature is 30.3 °C, and the ambient air humidity is 38%.

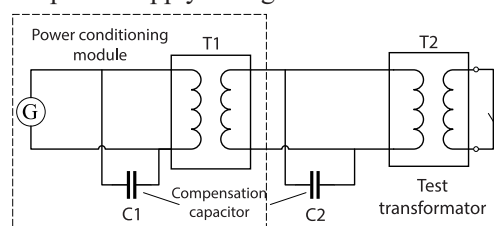


Figure 7. Schematic diagram of the experimental circuit of the short circuit method

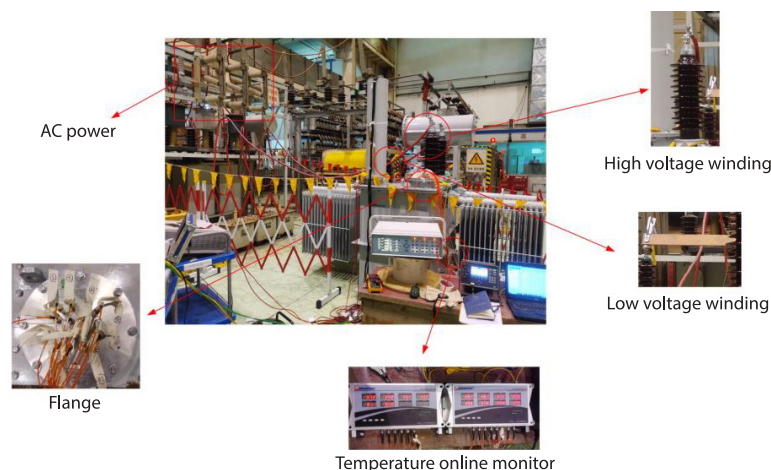


Figure 8. Field wiring diagram of the temperature rise experiment transformer

Selection and installation of optical fiber sensing temperature probe

As a traditional temperature measuring instrument, thermocouple probes have low cost, and are widely used in temperature measurement of various equipment. In [16] uses a

K-type thermocouple probe to monitor the temperature rise of the center coil of an air-dried power transformer online. However, the transformer is in the multi-field co-coupling action of electromagnetic-thermal-fluid field in actual work. When the thermocouple probe is introduced to measure temperature, the metal end of the probe will be interfered by the electromagnetic field, which arises the induction heating causing local overheating. Therefore, the accurate value of measuring point cannot be obtained correspondingly. In order to achieve real-time and obtain accurate temperature measurement of transformer windings, this experiment uses temperature optical fiber sensor based on rare-earth fluorescent materials to monitor the temperature measurement points in real time. The temperature measurement principle of the optical fiber sensor is to test the real-time temperature of the current environment by analyzing the length of the fluorescence afterglow lifetime. The time constant of afterglow decay is a single-valued function of temperature [17].

In order to verify the accuracy of the calculation results of the simulation model, the corresponding optical fiber probes were buried between the turns of the windings on both sides in this experiment, and one optical fiber probe was embedded at 18% of the winding axial height (the height of the oil inlet), two at 72% (the temperature concentration position in the upper part of the winding), and three fiber optic probes are embedded at 96% (the hot spot position of low voltage winding calculated in the simulation model). The temperature data is refreshed every 30 seconds at the beginning of the experiment for half an hour and then refreshed every 5 minutes. When the temperature rise rate of change is less than 1°C per hour, the transformer is considered to have reached the thermal equilibrium state. Among them, fig. 9(a) is a schematic diagram of the optical fiber temperature measurement wiring, and the details of the fiber lay-out inside the winding are shown in fig. 9(b).

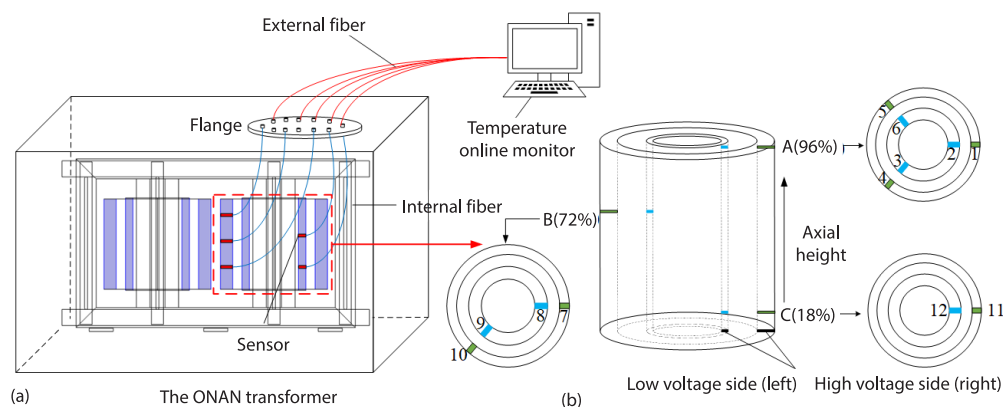


Figure 9. Schematic diagram of temperature measurement system of temperature optical fiber sensor; (a) schematic diagram of optical fiber temperature measurement and (b) optical fiber laying diagram inside the windings

Test data comparison and verification

Figures 10(a)-10(c) is a comparison diagram of the temperature rise test high voltage winding and low voltage winding internal optical fiber temperature point monitoring data. It can be seen from fig. 10 that when the test prototype reaches thermal equilibrium, the temperature values of optical fiber monitoring Points 2, 3, and 6 are 91.7 °C, 88.8 °C, and 89.9 °C, respectively. The average temperature is 90.14 °C, the corresponding simulation calculation value is 89.1 °C, and the relative error is 1.17%. The temperature values of monitoring Points 1,

4, and 5 are 85.2 °C, 84.5 °C, and 81.6 °C, respectively. Among them, the temperature data of Probe 4 fluctuates greatly. The possible reason is that the guiding effect of the surrounding oil baffle accelerates the oil flow around the probe, see fig. 5, causing the probe to loosen and the monitoring data fluctuates significantly. Therefore, in this paper, select the average temperature of Probes 1 and 5 (84.85 °C) as the test temperature, the corresponding simulation calculation value is 86.6 °C, and the relative error is 2.02%. The experiment monitoring temperature of middle measurement Points 8 and 9 are, respectively 83.3 °C and 83 °C, the average temperature is 83.15 °C. The corresponding simulation value is 85.2 °C, and the relative error is 2.41%. Correspondingly, the steady-state temperature of measurement Points 7 and 10 is 77.8 °C and 78.4 °C, the average temperature is 78.1 °C. The simulation value is 76.2 °C, and the relative error is 2.49%. The temperature of the monitoring Points 11 and 12 at the lower ends of the windings on both sides are 68.1 °C and 73.5 °C, respectively. The simulation values of this characteristic point are 68.9 °C and 76 °C, and the relative errors are 1.16% and 3.30%. The comparison result of the simulation value is shown in fig. 10(d).

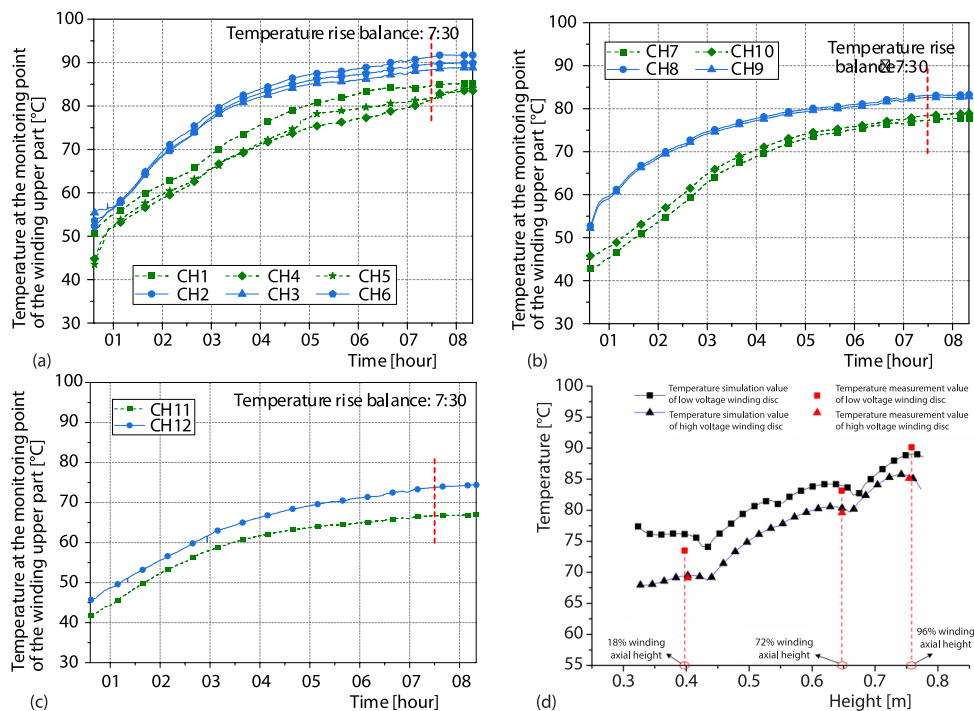


Figure 10. Comparison of temperature measurement data between the windings;
(a) comparison data of the winding upper part, (b) comparison data of the winding middle part, (c) comparison data of the winding lower, and (d) comparison of temperature measured and simulated values

In addition, combined with relevant transformer parameters, the empirical formula [18] can be used to calculate hot spot temperature rise. The results are shown in the tab. 3. According to the comparison of the results in fig. 10(d) and tab. 3, it can be seen that the result calculated by the coupling model constructed in this paper are more accuracy than those calculated by the empirical formula method, and the relative error less than 3.3%. Therefore, the validity and feasibility of the model are verified.

Table 3. Comparison of temperature results of empirical formula method, this method and experimental measurement

Temperature [°C]	Calculation method		Test measurement	Relative error [%]	
	Empirical formula	Method of this article		δ_e	δ_m
Low voltage winding hot spot	94.6	89.1	90.14	4.95	1.15
High voltage winding hot spot	90.7	86.6	—	6.89	—

Conclusions

In this paper, considering the hysteresis of the oil flow in the transverse oil passage between the winding turns and the guiding effect of the oil baffle, an electromagnetic-thermal-fluid coupling simulation model of the ONAN transformer is established. Therefore, the distribution characteristics of the temperature field and fluid field of the inner winding of the transformer are calculated. A temperature rise test of experiment prototype with a rated capacity of 800 kVA was carried out to verify the simulation results. The main conclusions are as follows.

- The hot spot of the ONAN transformer is located at the third wire cake below the end of the low voltage winding (96% of the axial height of the winding) whose temperature rise is 58.8 °C, and the hot spot of the high voltage winding is located at the 93% of the axial height.
- There is oil flow lag in the transverse oil passage between the winding turns on both sides. The installation of the corresponding oil baffle can increase the oil flow velocity in the transverse oil passage by 12 times by forced driving, and the oil temperature difference on both sides of the oil baffle can reach 2.42 °C. It can be seen that the oil baffle heat dissipation optimization effect is remarkable.
- Through the short-circuit temperature rise test of the transformer experiment prototype, the experimental measured value and the corresponding sample point simulation value are compared and analyzed. The result shows that the relative error between the two is less than 3.3%, which verifies accuracy of the ONAN transformer electromagnetic-thermal-fluid coupling model proposed in this paper.

Acknowledgment

Funded by State Grid Corporation Headquarters Program (Project No. 5500-202017468A-0-0-00).

References

- [1] Tao, C., et al., Transition Mode from Overhead Transmission-Line to Cable of Different Voltage Levels, *Power and Energy*, 33 (2012), 6, pp. 590-592
- [2] Wu, S., Study and Evaluation of Clustering Algorithm for Solubility and Thermodynamic Data of Glycerol Derivatives, *Thermal Science*, 23 (2019), 5, pp. 2867-2875
- [3] Arabul A. Y., et al., Development of a Hot-Spot Temperature Calculation Method for the Loss of Life Estimation of an ONAN Distribution Transformer, *Electrical Engineering*, 100 (2018), 3, pp. 1651-1659
- [4] Arabul, A. Y., et al., Experimental Thermal Investigation of an ONAN Distribution Transformer by Fiber Optic Sensors, *Electric Power Systems Research*, 155 (2018), 100, pp. 320-330
- [5] Swift G., et al., A Fundamental Approach to Transformer Thermal Modelling – Part I: Theory and Equivalent Circuit, *IEEE Transactions on Power Delivery*, 16 (2001), 2, pp. 171-175
- [6] Wang, F., et al., Improved Thermal Circuit Model of Hot Spot Temperature in Oil-Immersed Transformer Based on Heat Distribution of Winding, *High Voltage Engineering*, 41 (2015), 3, pp. 895-901

- [7] Quan, Y., *et al.*, Transformer Hot-Spot Temperature Inversion Method Based on Streamline and Support Vector Regression, *Advanced Technology of Electrical Engineering and Energy*, 37 (2018), 11, pp. 23-31
- [8] Cordoba P. A., *et al.*, A 3-D Numerical Model of an ONAN Distribution Transformer, *Applied Thermal Engineering*, 148 (2019), Feb., pp. 897-906
- [9] Xu, D., *et al.*, Analysis of Winding Temperature Field under Dynamic Variable Load of Oil-Immersed Transformer, *Thermal Science*, 25 (2021), 4 Part B, pp. 3009-3019
- [10] Ruan, J., *et al.*, The HST Calculation of a 10 kV Oil-Immersed Transformer with 3-D Coupled-Field Method, *IET Electric Power Applications*, 14 (2020), 5, pp. 921-928
- [11] Torriano, F., *et al.*, Numerical Investigation of 3-D Flow and Thermal Effects in a Disc-Type Transformer Winding, *Applied Thermal Engineering*, 40 (2012), July, pp. 121-131
- [12] Liao, C., *et al.*, Comprehensive Analysis of 3-D Electromagnetic-Fluid-Thermal Field of Oil-Immersed Transformer, *Electric Power Automation Equipment*, 35 (2015), 9, pp. 150-155
- [13] Tao, W., *Numerical Heat Transfer*, Xi'an, Xi'an Jiaotong University Press, Xi'an, China, 2001
- [14] Zhang, J., *Advanced Heat Transfer*, Nanjing, Nanjing University of Aeronautics and Astronautics, Nanjing, China, 2015
- [15] Hu, Q., *Transformer Test Technology*, China Electric Power Press, Beijing, China, 2010
- [16] Moonhee, L., *et al.*, Temperature Distribution in Foil Winding for Ventilated Dry-Type Power Transformers, *Electric Power Systems Research*, 80 (2010), 9, pp. 1065-1073
- [17] Li, Y., *et al.*, Research on a Method for Optical Fiber Fluorescence Specture Temperature Measurement, *Sensor World*, 20 (2014), 11, pp. 23-26
- [18] ***, *Oil-Immersed Transformer Design Manual*, Shenyang Transformer Co., Ltd, Shenyang, China, 2002